Inorg. Chem. **2006**, *45*, 1935–1944

Synthesis and Theoretical Study of a Series of Dipalladium(I) Complexes Containing the $Pd_2(\mu\text{-}CO)_2$ Core

Sylvie Baig,[†,‡] Brigitte Richard,[†] Philippe Serp,[†] Claude Mijoule,[§] Khansaa Hussein,[⊥,#] Nathalie Guihéry,[⊥] Jean-Claude Barthelat,[⊥] and Philippe Kalck*[,†]

Laboratoire de Catalyse Chimie Fine et Polymères, Ecole Nationale Supériere d'Ingénieurs en Arts Chimiques et Technologiques (ENSIACET), 118 Route de Narbonne, F-31077 Toulouse Cedex, France, and CIRIMAT UMR CNRS/INPT/UPS, Ecole Nationale Supériere d'Ingénieurs en Arts Chimiques et Technologiques (ENSIACET), 118 Route de Narbonne, F-31077 Toulouse Cedex, France, and Laboratoire de Physique Quantique, IRSAMC (UMR 5626), Université Paul Sabatier, 118 route de Narbonne, 31062, Toulouse Cedex 4, France

Received June 6, 2005

The complex $[PBu_4]_2[Pd_2(\mu\text{-}CO)_2Cl_4]$ has been prepared in high yields by carbonylation of $[PBu_4]_2[Pd_2Cl_6]$. Methanol, potassium acetate, or CO readily reacted under ambient conditions to quantitatively afford a series of dipalladium(I) complexes, namely $[Pd_2(\mu\text{-}CO)_2Cl_3(OCH_3)]^{2-}$, $[Pd_2(\mu\text{-}CO)_2Cl_3(OC(O)CH_3)]^{2-}$, $[Pd_2(\mu\text{-}CO)_2Cl_3(CO)]^{-}$, and $[Pd_2(\mu\text{-}CO)_2Cl_2(OCH_3)(CO)]^{-}$, all of which have the $Pd_2(\mu\text{-}CO)_2$ core preserved. All these complexes have been characterized by infrared and NMR spectroscopies; the high ν_{CO} stretching wavenumbers observed and the diamagnetic character of these complexes prompted us to perform theoretical calculations to describe the electronic structure of the $Pd_2(\mu\text{-}CO)_2$ core and to gain an intimate description of the Pd–CO bonds. The pairing of the two lonely electrons of the Pd d^9 atoms is due to the delocalization along the CO bridging ligands.

1. Introduction

Reductive carbonylation of $PdCl_2$ has been known since 1926[1] and does not provide palladium(0) species that would be of low stability; it instead yields a palladium(I) chlorocarbonyl polymer $[PdCl(CO)]_n$[2] in which the palladium atoms are alternatively bridged by two COs and two chloro ligands.[3] The same material is produced via the formation of a mixed palladium(I)−palladium(II) $[Pd_4Cl_5(CO)_5]$ species upon $[Pd^{II}_2(\mu\text{-}Cl)_2Cl_2(CO)_2]$ carbonylation.[4,5] Similarly, the reaction of carbon monoxide with $[PdCl_4]^{2-}$ in aqueous acid solutions gives $[Pd^{I}_2(\mu\text{-}CO)_2Cl_4]^{2-}$.[6] This complex is also produced by the addition of ammonium chloride to $[PdCl(CO)]_n$.[3] The structure of this dipalladium(I) complex, originally proposed from infrared data, displays a centrosymmetrical $Pd_2(\mu\text{-}CO)_2$ core.[7] It contains two bridging CO ligands at high wavenumbers (1966 (m) and 1906 (s) cm^{-1}), compared to ca. 1800 cm^{-1} for classical bridged carbonyls.[7] Two important features arise from such a disposition of the chloro and carbonyl ligands around the two palladium centers: (i) the presence of a direct metal−metal bond, as suggested by the 2.69 Å distance between the two palladium atoms, and (ii) the high ν_{CO} wavenumbers, which should account for a weak back-donation.

Goggin and co-workers reported calculations on the frontier orbitals of $[Pd_2(\mu\text{-}CO)_2Cl_4]^{2-}$ that explain why the two CO ligands bridge the palladium(I) centers instead of the chloro ligands: the reason stems from unfavorable

* To whom correspondence should be addressed. E-mail: Philippe.Kalck@ensiacet.fr.

† Laboratoire de Catalyse Chimie Fine et Polymères, Ecole Nationale Supérieure d'Ingénieurs en Arts Chimiques Et Technologiques (ENSIACET).

‡ Present address: Degrémont SA, R&D Department, 183 avenue du 18 juin 1940, 92508 Rueil-Malmaison, France.

§ CIRIMAT UMR CNRS/INPT/UPS, Ecole Nationale d'Ingénieurs en Arts Chimiques Et Technologiques (ENSIACET).

⊥ Université Paul Sabatier.

Present address: Department of Chemistry, Faculty of Sciences, University Al-Baath, Homs, Syria.

(1) Manchot, W.; König, J. *Chem. Ber*. **1926**, *59*, 883.
(2) (a) Colton, R.; Farthing, R. H.; McCornick, M. J. *Aust. J. Chem.* **1973**, *26*, 2607. (b) Fischer, E. O.; Vogler, A. *J. Organomet. Chem.* **1965**, *3*, 161. (c) Schanbel, W.; Kober, E. *J. Organomet. Chem*. **1969**, *19*, 455. (d) Trieber, A. *Tetrahedron Lett.* **1966**, 2831.
(3) Goggin, P. L.; Mink, J. *J. Chem. Soc., Dalton Trans*. **1974**, 534.
(4) Calderazzo, F.; Belli Dell'Amico, D. *Inorg. Chem*. **1981**, *20*, 1310.
(5) Belli Dell'Amico, D.; Calderazzo, F.; Zandoña N. *Inorg. Chem.* **1984**, *23*, 137.
(6) Gel'man, A. D.; Meilakh, E. *Dokl. Akad. Nauk. SSSR* **1942**, *36*, 188.
(7) Goggin, P. L.; Goodfellow, R. J.; Herbert, I. R.; Orpen, A. G. *J. Chem. Soc., Chem. Commun*. **1981**, 1077.

10.1021/ic050910n CCC: $33.50
Published on Web 02/02/2006

interactions between filled π_d* and Cl orbitals.[7] Later, Kostic and Fenske carried out Hartree−Fock calculations to address the question of the metal−metal bonding in the $[Pd_2(\mu\text{-}CO)_2Cl_4]^{2-}$ complex.[8] They proposed that the Pd−Pd interaction occurs through space via the two bridging ligands. Additionally, two recent reviews focused on the structure and reactivity of various palladium complexes containing palladium−palladium bonds[9] and on theoretical calculations performed on palladium and platinum complexes.[10] Numerous metal−carbonyl compounds containing terminal CO ligands with ν_{CO} values higher than that of gaseous CO at 2143 cm^{-1} have been reviewed.[11] This survey points out that back-donation should be almost absent between the metal atom and the CO ligands.

As far as palladium(I) is concerned, the $Pd_2(\mu\text{-}CO)_2$ core has been found in complex polymeric structures that show a SO_3F unit interacting with three palladium atoms of three different $Pd_2(\mu\text{-}CO)_2$ units, with the ν_{CO} wavenumber reaching 2002 cm^{-1}.[12] Some dipalladium(I) complexes containing mono- or diphosphines present only one CO ligand. A semi-bridging carbonyl ligand has been reported for the $[Pd_2(\mu\text{-}CO)Cl_2(PEt_2Ph)_3]$ dimer.[13] In the A-frame complexes containing the $Pd_2(diphos)_2$ or $Pd_2(diars)_2$ moieties, considering the low ν_{CO} stretching wavenumbers near 1720 cm^{-1} and the Pd−C bond distances, we can better view the CO ligand as belonging to a dimetalloketone framework in which CO is σ bonded to the two palladium(II) centers.[14,15]

We were interested in the synthesis of the palladium(I) species that are generated during the catalytic carbonylation of 1,3-diacetoxy-but-2-ene in methanol, affording the linear dimethyl hex-3-ene dioate diester compound.[16] In the present study, dianionic complexes of the type $[PBu_4]_2[Pd_2(\mu\text{-}CO)_2Cl_3X]$, with X = Cl, OMe, and OAc, and, under a CO atmosphere, monoanionic derivatives of the type $[PBu_4][Pd_2(\mu\text{-}CO)_2Cl_2X(CO)]$, with X= Cl and OMe, have been isolated and characterized. An ab initio study of the $[Pd_2(\mu\text{-}CO)_2Cl_4]^{2-}$ complex has been carried out in order to show how the two open-shell Pd centers can lead to a diamagnetic configuration, which allowed for a complete DFT analysis to be carried out. Calculations have been performed on this complex and extended to the two complexes of palladium(I) that present terminal CO ligands, $[Pd_2(\mu\text{-}CO)_2Cl_3(CO)]^-$ and the hypothetical $[Pd_2(\mu\text{-}CO)_2Cl_2(CO)_2]$.

(8) Kostić, N. M.; Fenske, R. F. *Inorg. Chem.* **1983**, *22*, 666.
(9) Murahashi, T.; Kurosawa, H. *Coord. Chem. Rev.* **2002**, *231*, 207.
(10) Dedieu, A. *Chem. Rev.* **2000**, *100*, 543.
(11) Lupinetti, A. J.; Strauss, S. H.; Frenking, G. In *Progress in Inorganic Chemistry, Vol. 49*; Karlin, D. K., Ed.; Wiley & Son: New York, 2001; pp 1−112.
(12) Wang, C.; Bodenbinder, M.; Willner, H.; Rettig, S.; Trotter, J.; Aubke, F. *Inorg. Chem.* **1994**, *33*, 779.
(13) Feltham, R. D.; Elbaze, G.; Ortega, R.; Eck, C.; Dubrawski, J. *Inorg. Chem.* **1985**, *24*, 1503.
(14) (a) Colton, R.; McCormick, M. J.; Pannan, C. D. *J. Chem. Soc., Chem. Commun.* **1977**, 823. (b) Colton, R.; McCormick, M. J.; Pannan, C. D. *Austr. J. Chem.* **1978**, *31*, 823.
(15) Wink, D. J.; Creagan, B. T.; Lee, S. *Inorg. Chim. Acta* **1991**, *180*, 183.
(16) (a) Deweerdt, H.; Jenck, J.; Kalck, P. French patent 88/08 197, 1988. (b) Duprat, S.; Deweerdt, H.; Jenck, J.; Kalck, P. *J. Mol. Catal.* **1993**, *80*, L9.

2. Experimental Section

2.1. General Procedures. All manipulations were performed under a dry, oxygen-free, nitrogen, or argon atmosphere using standard Schlenk techniques. Dichloromethane was dried and distilled over CaH_2; toluene was distilled under argon over Na/benzophenone. Other organic solvents were used as received without any further purification. Carbon monoxide was purchased from Air Liquide (99.995 purity). Infrared spectra were recorded on a Perkin-Elmer model 1710 spectrometer. NMR spectra were recorded at 25 °C on a Bruker WM 250 MHz spectrometer. The ^1H and $^{13}C\{^1H\}$ resonances of the solvent were used as the internal standard, but the relevant chemical shifts are reported with respect to TMS.

2.2. Syntheses. Bis(tetrabutylphosphonium)-hexachlorodipalladium(II), $[PBu_4]_2[Pd_2Cl_6]$ (1). This complex was prepared from $PdCl_2$ (0.40 g, 2.20 mmol) and $[PBu_4]Cl$ (0.66 g, 2.20 mmol) in 60 mL of distilled toluene. The solution, heated under N_2 at 100 °C overnight, progressively turned from dark brown to dark red. After decantation, the yellow upper phase was eliminated and the red oily lower phase was dried in vacuo, affording a red powder. Recrystallization from a methyl-isobutyl-ketone (MIBK)−pentane bilayered mixture gave the desired product as red needles (1.90 g, 1.98 mmol, 90%). Elemental anal. Calcd for $C_{32}H_{72}Cl_6P_2Pd_2$: C, 40.70; H, 6.32; P, 6.56; Pd, 22.53. Found: C, 40.79; H, 7.12; P, 6.76; Pd, 22.32.

Bis(tetrabutylphosphonium)-tetrachlorodi(μ-carbonyl)dipalladium(I), $[PBu_4]_2[Pd_2(\mu\text{-}CO)_2Cl_4]$ (2). This complex was prepared by carbonylation at room temperature (CO bubbling in a flask equipped with a condenser, 20 min) of a solution of **1** (0.50 g, 0.52 mmol) in 50 mL of distilled dichloromethane. Upon bubbling, the solution progressively turned from dark red to lemon yellow. After solvent evaporation and recrystallization from a toluene−hexane bilayered mixture, **2** was obtained as yellow needles (0.35 g, 0.37 mmol, 72%). ^{13}C NMR (50.323 MHz, CD_2Cl_2, 25 °C): δ 193.2. IR (KBr): 1964 (w), 1903 (s) cm^{-1}. IR (CH_2Cl_2): 1968 (w), 1906 (s) cm^{-1}. Elemental anal. Calcd for $C_{34}H_{72}Cl_4O_2P_2Pd_2$: C, 43.92; H, 7.82; P, 6.66; Pd, 22.89. Found: C, 44.19; H, 8.35; P, 6.65; Pd, 23.24.

Bis(tetrabutylphosphonium)-trichloro(methoxy)di(μ-carbonyl)dipalladium(I), $[PBu_4]_2[Pd_2(\mu\text{-}CO)_2Cl_3(OCH_3)]$ (3). To a solution of **2** (0.50 g, 0.54 mmol) in 125 mL of MIBK was added 2 mL (49.4 mmol) of methanol at room temperature. The solution was stirred for 15 h, and the resulting product was recrystallized at −18 °C by the addition of pentane (10 mL). This compound was obtained as red needles (0.40 g, 0.43 mmol, 80%). ^1H NMR (200 MHz, $CDCl_3$, 25 °C): δ 1.57 (methoxy group). ^{13}C NMR (50.323 MHz, $CDCl_3$, 25 °C): δ 195.0 (bridged CO), 23.83 (methoxy group). IR (KBr): 1963 (w), 1905 (s) cm^{-1}. Elemental anal. Calcd for $C_{35}H_{75}Cl_3O_3P_2Pd_2$: C, 45.42; H, 8.17; P, 6.70; Pd, 22.93. Found: C, 44.86; H, 7.85; P, 6.76; Pd, 22.25.

Bis(tetrabutylphosphonium)-(acetoxy)trichlorodi(μ-carbonyl)dipalladium(I), $[PBu_4]_2[Pd_2(\mu\text{-}CO)_2Cl_3(OOCCH_3)]$ (4). To a solution of **2** (0.50 g, 0.54 mmol) in MIBK (125 mL) was added 53 mg (0.54 mmol) of potassium acetate at room temperature. The solution was stirred for 15 h, and the compound was recrystallized at −18 °C by the addition of pentane (10 mL). This compound was obtained as red needles (0.40 g, 0.405 mmol, 75%). ^1H NMR (200 MHz, $CDCl_3$, 25 °C): δ 1.67 (acetoxy group). IR (KBr): 1963 (w), 1905 (s), 1647 (w) cm^{-1}. Elemental anal. Calcd for $C_{36}H_{75}Cl_3O_4P_2Pd_2$: C, 45.36; H, 7.93; P, 6.50; Pd, 22.33. Found: C, 44.22; H, 7.98; P, 6.68; Pd, 22.39.

Tetrabutylphosphonium-(carbonyl)trichlorodi(μ-carbonyl)dipalladium(I), $[PBu_4][Pd_2(\mu\text{-}CO)_2(CO)Cl_3]$ (5). This complex

was prepared by carbonylation at room temperature (CO bubbling in a flask equipped with a condenser, 20 min) of a solution of **1** (0.50 g, 0.52 mmol) in 50 mL of distilled dichloromethane. Upon bubbling, the solution progressively turned from dark red to lemon yellow. After 20 min, the condenser was removed, and CH_2Cl_2 was completely evaporated under further CO bubbling. The solid residue was recrystallized from a toluene−hexane bilayered mixture. The compound was obtained as yellow needles (0.20 g, 0.31 mmol, 60%). ^{13}C NMR (50.323 MHz, CD_2Cl_2, 25 °C): δ 192.9 (bridged CO), 168 (terminal CO). IR (KBr): 2114 (vs), 1964 (w), 1903 (s) cm^{-1}. IR (CH_2Cl_2): 2133 (vs), 1968 (w), 1907 (s) cm^{-1}. Elemental anal. Calcd for $C_{19}H_{36}Cl_3O_3PPd_2$: C, 34.43; H, 7.42. Found: C, 40.55; H, 7.40. This discrepancy between calculated and experimental values results from the presence of $[PBu_4]Cl$, which cocrystallizes with complex **5**. When 25% of $[PBu_4]Cl$ is considered in addition to **5**, the calculated values are C, 40.31; H, 7.68.

Tetrabutylphosphonium-(carbonyl)dichloro(methoxy)di(μ-carbonyl)dipalladium(I), $[PBu_4][Pd_2(CO)(\mu\text{-}CO)_2Cl_2(OCH_3)]$ (6). To a solution of **2** (0.50 g, 0.54 mmol) in dichloromethane (125 mL) was added 2 mL (49.4 mmol) of methanol at room temperature. Upon CO bubbling of the solution at 35 °C, IR spectra of the solution showed the appearance of a ν_{CO} band at 2120 cm^{-1}. The complex was isolated as a yellow powder by solvent and unreacted methanol evaporation under CO flow and by further dissolution in toluene followed by the addition of pentane (0.22 g, 0.32 mmol, 61%). ^{1}H NMR (200 MHz, $CDCl_3$, 25 °C): δ 1.60 (methoxy group). ^{13}C NMR (50.323 MHz, $CDCl_3$, 25 °C): δ 193.0 (bridged CO), 163.2 (terminal CO), 24.03 (acetoxy group). IR (KBr): 2120 (s), 1963 (w), 1903 (s) cm^{-1}.

3. Computational Details

Concerning the multireference calculations, the orbitals were optimized through the complete active space self-consistent field (CASSCF) procedure for the ground state using the MOLCAS package.[17] Then, to include the dynamic correlation, we performed a difference dedicated configuration interaction (DDCI)[18] calculation using the CASDI package.[19] In this CI, which is in principle designed for the treatment of energy differences between states of the same CAS and at the same geometry, all the singly excited determinants as well as the doubly excited determinants that differ by less than four orbitals (outside of the CAS) were treated variationally. It is worthwile to notice that the DDCI variational treatment is crucial in order to accurately take into account the most important part of the dynamic correlation. Finally, to obtain reliable energy differences between various geometries, the last class of doubly excited determinants (i.e., those in which two inactive electrons are promoted to two virtual orbitals) was treated perturbatively using the CASPT2 algorithm.

For palladium, quasirelativistic energy-adjusted pseudopotentials determined by Dolg et al.[20] were used to represent the Pd-like core. The 18 electrons corresponding to the 4s, 4p, 4d, and 5s atomic orbitals were described by a (8s, 7p, 6d) primitive set of Gaussian functions contracted to (6s, 5p, 3d). To estimate the contribution of *f* functions to the correlation of palladium d electrons, we performed an additional calculation with one *f* function on palladium atoms. The core electrons of chlorine, oxygen, and carbon atoms were represented by a pseudopotential determined by Barandiaran and Seijo.[21] The seven valence electrons of chlorine were described by (7s, 7p, 1d) primitive functions contracted to (2s, 2p, 1d).[21] The six valence electrons of oxygen were described by (5s, 6p, 1d) primitive functions contracted to (1s, 2p, 1d),[21] and the four valence electrons of carbon by (5s, 5p, 1d) primitive functions contracted to (2s, 2p, 1d).[21]

DFT calculations were performed with the Gaussian 98 series of programs[22] using the non-local hybrid functionals denoted as B3LYP[23] and B3PW91.[24] In these calculations, we used for Pd the same pseudopotential and basis sets as those used previously. Standard pseudopotentials developed in Toulouse were used to describe the atomic cores of carbon, oxygen, and chlorine.[25] A double-ζ plus polarization valence basis set was employed for carbon, oxygen, and chlorine (the d-type polarization function exponents were 0.80, 0.85, and 0.65, respectively). To take into account the anionic character of the complexes, we also used a more extended basis containing p diffuse functions on chlorines.

The geometries of the different species under consideration were fully optimized using an analytic gradient. The harmonic vibrational wavenumbers of the different stationary points on the potential-energy surface (PES) have been calculated at the same level of theory in order to identify the local minima as well as to estimate the corresponding zero-point energy (ZPE). The nature of the palladium−carbonyl bonds was analyzed using natural bond orbital (NBO) calculations.[26]

4. Results and Discussion

4.1. Synthesis and Characterization of the Dipalladium(I) Complexes. A convenient way to prepare the tetrachlorodi(μ-carbonyl)dipalladium dianion in high yield is to start from $[Pd_2Cl_6]^{2-}$. Usually, when employing ammonium salts, we obtained oily compounds; with $[PBu_4]^+$ as the counterion, we could obtain microcrystalline materials. However, all of the compounds investigated in this study containing this cation crystallized as very small needles

(17) Roos, B. O.; Taylor, P.; Siegbahn, P. *Chem. Phys.* **1980**, *48*, 157.
(18) Miralles, J.; Castell, O.; Caballol, R.; Malrieu, J. P. *Chem. Phys.* **1993**, *172*, 33.
(19) Ben Amor, N.; Maynau, D. *Chem. Phys. Lett.* **1998**, *286*, 211.
(20) Andrea, D.; Haeussermann, U.; Dolg, M.; Stoll, H.; Preuss, H. *Theor. Chim. Acta* **1990**, *77*, 123.
(21) Barandiaran, Z.; Seijo, L. *Can. J. Chem.* **1992**, *70*, 409.
(22) Frisch, M. J.; Trucks, G. W.; Schlegel, H. B.; Scuseria, G. E.; Robb, M. A.; Cheeseman, J. R.; Zakrzewski, V. G.; Montgomery, J. A., Jr.; Stratmann, R. E.; Burant, J. C.; Dapprich, S.; Millam, J. M.; Daniels, A. D.; Kudin, K. N.; Strain, M. C.; Farkas, O.; Tomasi, J.; Barone, V.; Cossi, M.; Cammi, R.; Mennucci, B.; Pomelli, C.; Adamo, C.; Clifford, S.; Ochterski, J.; Petersson, G. A.; Ayala, P. Y.; Cui, Q.; Morokuma, K.; Salvador, P.; Dannenberg, J. J.; Malick, D. K.; Rabuck, A. D.; Raghavachari, K.; Foresman, J. B.; Cioslowski, J.; Ortiz, J. V.; Baboul, A. G.; Stefanov, B. B.; Liu, G.; Liashenko, A.; Piskorz, P.; Komaromi, I.; Gomperts, R.; Martin, R. L.; Fox, D. J.; Keith, T.; Al-Laham, M. A.; Peng, C. Y.; Nanayakkara, A.; Challacombe, M.; Gill, P. M. W.; Johnson, B.; Chen, W.; Wong, M. W.; Andres, J. L.; Gonzalez, C.; Head-Gordon, M.; Replogle, E. S.; Pople, J. A. *GAUSSIAN 98*, Revision A.11, Gaussian, Inc.: Pittsburgh, PA, 2001.
(23) (a) Becke, A D. *J. Chem. Phys.* **1993**, *98*, 5648. (b) Lee, C.; Yang, W.; Parr, R. G. *Phys. Rev. B* **1988**, *37*, 785.
(24) Perdew, J. P.; Wang, Y. *Phys. Rev. B* **1992**, *45*, 13244.
(25) Bouteiller, Y.; Mijoule, C.; Nizam, M.; Barthelat, J.-C.; Daudey, J.-P.; Pélissier, M.; Silvi, B. *Mol. Phys.* **1988**, *65*, 2664.
(26) Reed, A. E.; Curtiss, L. A.; Weinhold, F. *Chem. Rev.* **1988**, *88*, 899.

Scheme 1. Reactivity of Complex **2** $[Pd_2(\mu\text{-}CO)_2Cl_4]^{2-}$

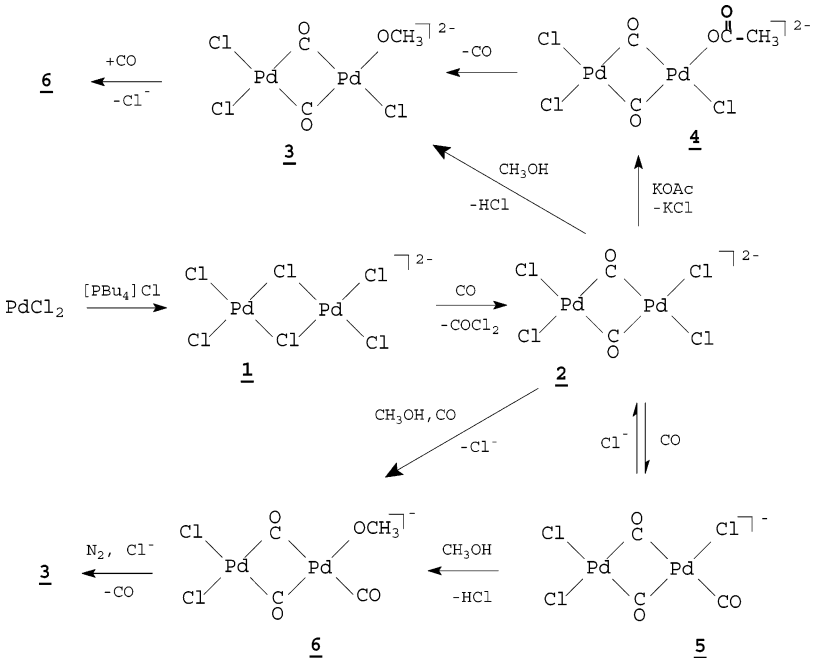

unsuitable for X-ray diffraction analysis. Thus, adding $[PBu_4]$-Cl to $PdCl_2$ leads to the quantitative formation of $[PBu_4]_2[Pd_2$-$Cl_6]$ **1** as a red solid. Bubbling carbon monoxide at room temperature through a CH_2Cl_2 solution of **1** very quickly gives a yellow solution, the infrared spectra of which show a short-lived ν_{CO} at 2134 cm^{-1}, and the growth of the two ν_{CO} bands of $[PBu_4]_2[Pd_2(\mu\text{-}CO)_2Cl_4]$ **2** at 1968 (w) and 1906 (s) cm^{-1}. The intermediate species formed is $[PdCl_3(CO)]^-$, which could not be isolated under these conditions, as the reduction reaction is complete in less than 5 min. Facile isolation of $[PdCl_3(CO)]^-$ was possible starting from $[PPN]_2$-$[Pd_2Cl_6]$. The addition of pentane to MIBK solutions of **2** gave yellow crystals in a 72% yield. For the centrosymmetric $Pd_2(\mu\text{-}CO)_2$ core, the symmetric ν_{CO} mode is expected to be infrared inactive. However, in either solution or the solid state, the presence of a ν_{CO} band of weak intensity at 1968 and 1964 cm^{-1}, respectively, is consistent with a small puckering toward a C_{2v} local symmetry. Conversely, Goggin et al.[7] observed a weak ν_{CO} band in solution, but in the solid state the absence of the ν_{CO} symmetric mode is consistent with the X-ray crystal structure of $[NBu_4]_2$ $[Pd_2(\mu\text{-}CO)_2Cl_4]$.

Complex **2** is a reactive species that may undergo different substitution reactions while maintaining the integrity of the $Pd_2(\mu\text{-}CO)_2$ core; its reactivity is displayed in Scheme 1. The addition of 100 equiv of methanol or 1 equiv of potassium acetate in MIBK solution induces selective substitution of one chloro ligand, to yield $[PBu_4]_2[Pd_2(\mu\text{-}CO)_2Cl_3(OMe)]$ **3** and $[PBu_4]_2[Pd_2(\mu\text{-}CO)_2Cl_3(OC(O)CH_3]$ **4**, respectively. The latter complex shows a low stability in solution and, for instance, the ^{13}C NMR spectra cannot be recorded, because of a rapid evolution toward **3**. Thus, decarbonylation occurs, presumably after an isomerization process from the acetoxy to a methoxycarbonyl group. Complex **4** shows two ν_{CO} bands in KBr pellets at 1963 (w) and 1905 (s) cm^{-1}, very close to those of **2** and **3**, and also shows a band of weak intensity at 1647 cm^{-1} that corresponds to the acetoxy group.

Table 1. IR and NMR Characterization of Complexes **2**, **3**, **5**, and **6**

	ν_{CO} (cm^{-1})[a]		δ ^{13}CO (ppm)[b]	
complex	bridging	terminal	bridging	terminal
2	1964 (w), 1903 (s)		193	
3	1963 (w), 1905 (s)		195	
5	1964 (w), 1903 (s)	2114 (vs)	193	168
6	1963 (w), 1903 (s)	2120 (s)	193	163

[a] In KBr. [b] In $CDCl_3$.

Moreover, when CO is further bubbled through CH_2Cl_2 solutions of **2**, a third ν_{CO} band appears at 2133 cm^{-1}, which is indicative of a terminal CO ligand. Evaporation of CH_2-Cl_2 under CO and crystallization of this novel complex in toluene−pentane solutions saturated with CO leads to the isolation of $[PBu_4][Pd_2(\mu\text{-}CO)_2Cl_3(CO)]$ **5** as a yellow powder. This reaction is reversible and, if $[PBu_4]Cl$ is still present in solution, **5** gives back **2** under a dinitrogen atmosphere. Furthermore, the evolution of **3** upon CO bubbling, or the carbonylation of **2** when the solution contains 10 equiv of methanol, provides $[PBu_4][Pd_2(\mu\text{-}CO)_2$-$Cl_2(OMe)(CO)]$ **6**. As in the case of **5**, if $[PBu_4]Cl$ is still present in solution, **6** gives back **3** under dinitrogen. As we detected in solution a terminal ν_{CO} band at 2134 cm^{-1} during the decarbonylation of **4**, we suppose reasonably that the methoxy group and the terminal CO ligand in **6** are in a mutual cis position on the same palladium center, as they would arise from the decarbonylation of a methoxycarbonyl group. Indeed, in **4**, the acetoxy group needs to be isomerized into the methoxycarbonyl group before decarbonylation.

Infrared and ^{13}C NMR data (see Table 1) reveal that the terminal CO ligand in **5** or **6**, as well as the bridging COs of **2**, **3**, **5**, and **6**, are unaffected by modifications in the remaining part of the coordination sphere. However, it is worth mentioning that although we expect two slightly different chemical shifts in ^{13}C NMR for the CO bridging ligands of **3**, **4**, **5**, and **6**, spectra at room temperature present

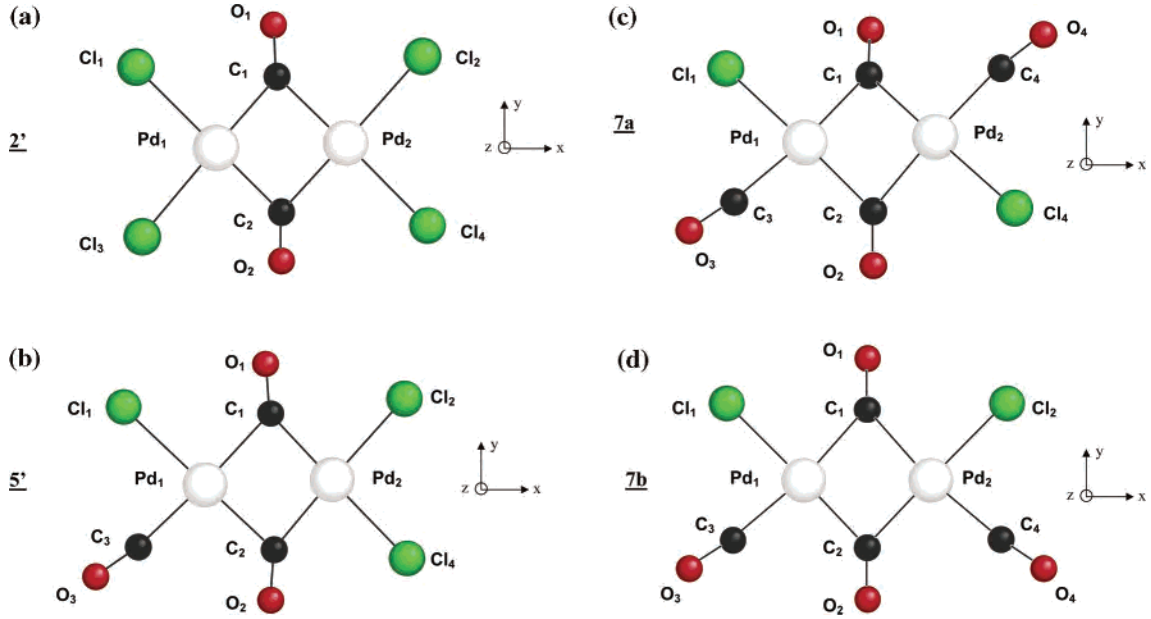

Figure 1. B3LYP-optimized geometries of compounds **2′**, **5′**, **7a**, and **7b**.

a single resonance near 195 ppm. Presumably, a fluxional process exists that induces the equivalence of the two COs. Moreover, complexes **2**−**4** are dianionic, whereas **5** and **6** are monoanionic. High stretching wavenumbers are observed for both terminal and bridging CO ligands. In the X-ray crystal structure of **2** ($[NBu_4]^+$ instead of $[PBu_4]^+$) determined by Goggin and co-workers, a short palladium−palladium distance of 2.697(3) Å has been determined.[6,9] The environment of the two d^9 metal centers is square planar, although a small tetrahedral distortion (around 9°) is present. The authors have also calculated the frontier orbitals in order to understand the reason the CO ligands occupy the bridging positions instead of the two chloro ligands.

To gain further insight into the nature of the bonding in the **2** and **5** d^9−d^9 dimers and to understand why the ν_{CO} stretching wavenumbers are so high, we have performed a theoretical study on the two ionic units of these species (**2′** and **5′** in the absence of cation) by using several quantum chemistry methods. This analysis has been extended to the two isomers of the neutral dimer that would contain two terminal CO ligands in addition to the two bridging carbonyl groups $[Pd_2(\mu\text{-}CO)_2Cl_2(CO)_2]$ **7a** and **7b**.

4.2. Theoretical studies. 4.2.1. Role of the electronic correlation in $[Pd_2(\mu\text{-}CO)_2Cl_4]^{2-}$ 2′. A theoretical study of palladium(I) dianion **2′** has been performed using both the density functional theory and highly correlated ab initio methods such as multireference configuration interactions, including singly and doubly excited determinants. The dianion is represented in Figure 1, with the Cartesian axis system. As it will be shown hereafter, the use of correlated descriptions was compulsory. The compound under study is a palladium(I) dimer so that each Pd brings a lonely electron to the system. To elucidate the electronic structure of the dianion, the question of the pairing of these two electrons must be addressed. Whereas analogue organometallic compounds are generally paramagnetic, the present Pd(I) dianion happens to be diamagnetic from experimental data. Nevertheless, the relevance of a single determinant description is not guaranteed. The given theoretical treatment used herein follows a strategy that has been shown to produce reliable results for magnetic systems.[27−29] These compounds are known to be particularly difficult to describe because both the nondynamic and the dynamic correlations play an important role on their electronic structure.

First of all, to allow the two electrons to be paired or not, it is necessary to use a multireference treatment. The ligand field is responsible for a degeneracy removal of the d orbitals of the Pd atoms; the two d_{xy} orbitals of the Pd atoms are the most destabilized orbitals and bear these two electrons. To allow a charge fluctuation between these orbitals, the two molecular orbitals essentially built from these atomic orbitals have been set to an active state in the CASSCF procedure.

Three different geometries of **2′** have been studied, i.e., the planar crystallographic one[7] and two theoretical geometries optimized at the restricted DFT/B3LYP level of calculation. We first carried out a geometry optimization keeping the D_{2h} symmetry constraint. A vibrational analysis has shown that this D_{2h} structure presents two imaginary wavenumbers and does not correspond to a local minimum on the DFT PES. Another geometry of C_{2v} symmetry was obtained through a fully relaxed optimization. The C_{2v} B3LYP resulting structure does not present any imaginary wavenumber and corresponds to a true minimum. It is represented in Figure 1, and the corresponding geometrical parameters are given in Table 2. Notice that geometry optimizations carried out at the CASSCF level led to four dissociated fragments, namely two carbonyl groups and two $PdCl_2^-$ anions. On the contrary, when including the dynamic correlation (CAS-DDCI+PT2), energies of compound **2′** in

(27) de P. R. Moreira, I.; Illas, F.; Calzado, C. J.; Sanz, J. F.; Malrieu, J. P.; Ben Amor, N.; Maynau, D. *Phys. Rev. B* **1999**, *59*, R6593.
(28) Castell, O.; Caballol, R. *Inorg. Chem* **1999**, *38*, 668.
(29) Calzado, J. C.; Cabrero, J.; Malrieu, J. P.; Caballol, R. *J. Chem. Phys.* **2002**, *116*, 2728.

Table 2. X-ray Structural Data and DFT-Optimized Geometries for $[Pd_2(\mu\text{-}CO)_2Cl_4]^{2-a}$

		DFT optimizations		
	X-ray[b]	B3LYP D_{2h}	B3LYP C_{2v}	B3PW91 C_{2v}
Pd_1-Pd_2	2.697(3)	2.866	2.750	2.709
Pd_1-C_1	1.994(9)	1.978	2.033	2.011
C_1-O_1	1.140(10)	1.175	1.167	1.168
Pd_1-Cl_1	2.372(4)	2.500	2.445	2.421
$Pd_1-C_1-Pd_2$	85.2(3)	92.8	85.1	84.7
$Pd_1-C_1-O_1$		133.6	137.1	137.3
$C_1-Pd_1-C_2$		87.2	90.3	90.7
$Cl_1-Pd_1-Cl_3$		108.2	93.4	93.0
$Cl_1-Pd_1-C_1$		115.2	88.1	88.1
$C_1-Pd_1-Pd_2-C_2$		180.0	148.4	148.5

[a] Distances are in Å and angles in degrees. [b] X-ray data from ref 7.

the three geometries of interest are lower than the energy of the dissociated fragments, showing that this compound is stable. As will be shown later, the calculated properties of this compound at the B3LYP− optimized C_{2v} geometry are in good agreement with the experimental data. A slightly better agreement is obtained by using the B3PW91 functional. Furthermore, the extension of the basis set by including p diffuse functions on chlorines leads to the same conformational structure, the largest changes being less than 0.01 Å for bond lengths and 0.1° for bond angles. One way to evaluate the relevance of the optimized geometries at the B3LYP level is to compare the energy differences between both geometries at two different levels of theory. Whereas the energy difference between these two geometries is 28 kcal mol^{-1} at the B3LYP level, it is 25 kcal mol^{-1} at the CAS-DDCI+PT2 level, showing an overall good agreement between the two approaches. It should be noticed that electron correlation is responsible for the stability of this compound.

The other part of the analysis deals with the electronic structure of this compound. Its diamagnetic character is confirmed by the CASSCF calculations, the energy difference between the singlet and the triplet states being 2.16 eV for the C_{2v} optimized geometry. The corresponding active orbitals b_1 and a_2 are represented in Figure 2. The occupation numbers of the orbitals a_2 and b_1 are 1.832 and 0.168, respectively, at the CASSCF level. The a_2 orbital presents a nonbonding character between the two d_{xy} atomic orbitals and a bonding character between the d_{xy} and the π^* orbitals localized on the CO ligand. This latter interaction is responsible for the large stabilization of this orbital compared to the other one, which results in a quasidouble occupancy of the a_2 orbital. On the contrary, the b_1 orbital, which is bonding between the two d_{xy} orbitals, is destabilized by the antibonding interaction with the σ doublet of the carbons, and its final occupation number is rather small. The partial pairing of the two electrons is therefore attributable to the interaction of the Pd atoms through the bridging ligands, the resulting σ orbital being delocalized between these various atoms. It is worth mentioning that this orbital results from a π overlap between the two d_{xy} orbitals of the Pd atoms and a σ overlap between these d_{xy} orbitals and the π^* orbitals of the CO groups.

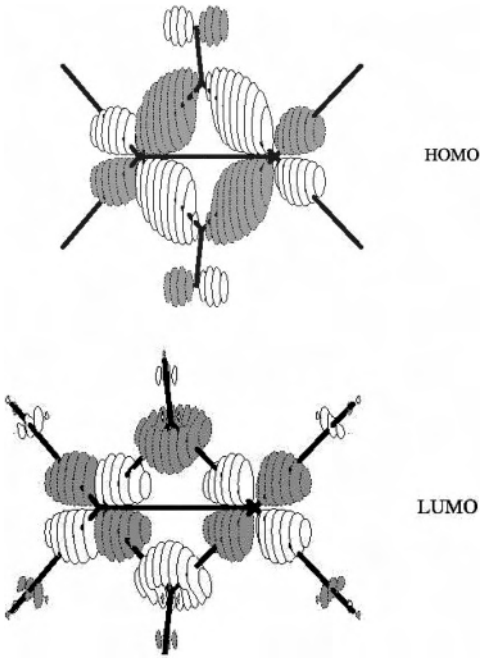

Figure 2. Highest occupied molecular orbital (HOMO) a_2 and lowest unoccupied molecular orbital (LUMO) b_1 optimized at the CASSCF level for the ground state of **2′**.

Nevertheless, the multireference character of the wave function is not negligible. The energy of the single reference wave function is higher than that of the multireference function by 0.97 eV. This result is confirmed by the unusually large coefficient (0.29) of the determinant in which the two electrons occupy the b_1 orbital. For analysis purposes, it is possible to perform a rotation of the delocalized molecular orbitals in order to obtain Pd-centered orthogonal orbitals (essentially spanned by the d_{xy} orbitals). The importance of the nondynamic correlation can be measured by the weight of the neutral valence bond (VB) determinants (Pd(I)−Pd(I)) compared to that of the ionic VB determinants (Pd(0)−Pd(II)). This weight is equal to 0.5 for both ionic and neutral VB forms in a single reference wave function. The CASSCF calculations dramatically reduce the weight of the ionic forms to 0.22.

Let us now analyze the role of the dynamic correlation. The occupation numbers of the natural orbitals obtained from the DDCI wave function are 1.89 and 0.10. The coefficient of the di-excited determinants (in which the two electrons occupy the b_1 orbital) is reduced to 0.12, whereas the coefficient of the dominant determinant is 0.92 and the weight of the ionic VB forms is now 0.33 (this value is not significantly altered by adding *f* functions on each palladium atom). As usually observed, the dynamic correlation increases the weight of the ionic forms, with the dynamic polarization allowing their relaxation (for a more detailed discussion see, for instance, ref 30). The effect of the dynamic correlation decreases the multireference character of the valence part of the wave function. This system is particularly interesting from a theoretical point of view, because although it is not

(30) Guihéry, N.; Malrieu, J. P.; Evangelisti, S.; Maynau, D. *Chem. Phys. Lett.* **2001**, *349*, 555.

a magnetic system, its description requires the inclusion of both nondynamic and dynamic correlations. Although the nondynamic correlation is not negligible, a DFT-type treatment seems to give reliable results.

4.2.2. Vibrational Analysis at the DTF Level. At the B3LYP level of calculation, a general study of the Pd(I) complexes dianion $[Pd_2(\mu\text{-}CO)_2Cl_4]^{2-}$ **2′**, monosubstituted anion $[Pd_2(\mu\text{-}CO)_2Cl_3(CO)]^-$ **5′**, and neutral disubstituted $[Pd_2(\mu\text{-}CO)_2Cl_2(CO)_2]$ **7a** (trans) and **7b** (cis), is presented in the following way: we first determined the equilibrium geometry for each complex. We can already note that concerning the disubstituted complexes **7a** and **7b**, the trans and cis geometries are very close in energy, the trans conformation **7a** being more stable by only 0.96 kcal mol^{-1}. Second, the relative strengths of the various bonds are estimated and compared through the values of the Wiberg bond indices. In the same way, the properties of the charge distributions in the complexes are analyzed by using the natural bond orbital (NBO) method, and more specifically, the donation and back-donation processes between the palladiums and the carbonyls are investigated. Vibrational wavenumbers of the bridging and terminal COs are calculated, and the localization of the corresponding normal modes is analyzed in order to explain the relative intensities of the bands in the IR spectra. Finally, a synthesis of all the previous results is made in order to show their strong correlations.

Geometrical Structures. Projections in the *xOy* plane of the dimeric d^9 Pd(I) dianion **2′** as well as of its substituted compounds are represented in Figure 1. The *x* axis lies along the Pd−Pd line, and the *y* axis along the carbon atoms of the bridging carbonyls (C_1 and C_2). All geometrical parameters are summarized in Table 2 (for compound **2′**) and in Table 3 (for compounds **5′**, **7a**, and **7b**). First, we must mention that none of the compounds are planar; more particularly, the $Pd_2(\mu\text{-}CO)_2$ core is puckered, and the corresponding dihedral angle is close to 150° (see Table 1). It results that the symmetry groups are C_{2v} for **2′** (*z* is the C_2 axis), C_1 for **5′**, C_2 for **7a** (*z* is the C_2 axis), and C_s for **7b** (*yz* is the σ plane). As will be shown later, this explains why the intensities of both vibrations related to the bridging carbonyls are non-zero in all complexes. IR experimental results for **2′** and **5′** confirm this kind of conformation.

Pd−Pd distances are nearly the same in all compounds (2.7−2.8 Å), and a priori should be compatible with a direct metal−metal bond. However, the CASSCF calculations (see previous section) have shown that this is not a correct description. Concerning the C−O bond lengths of the carbonyl ligands, we have to distinguish between bridging and terminal positions. The lengthening of the C−O bond with respect to the value calculated for free CO at the same level of theory (1.141 Å) is significant for the bridging COs (about 0.02 Å), whereas the CO bond length is unchanged for the terminal COs. We may then expect that the bond strength in a bridging CO is weakened under complexation, resulting in a decreasing of the CO vibrational wavenumber with respect to the free CO. The Pd−Cl bond lengths decrease uniformly when going from **2′** to **5′**, then to **7a** or **7b**, and are thus more related to the electronic charge of the compound than to the number of terminal COs.

Table 3. B3LYP-Optimized Geometries of Pd(I) Compounds (distances in Å, angles in deg)

	5′	**7a**	**7b**
symmetry	C_1	C_2	C_s
	Bond Lengths		
Pd_1-Pd_2	2.760	2.777	2.789
Pd_1-C_1	2.147	2.060	2.092
Pd_1-C_2	2.098	2.079	2.058
Pd_2-C_1	2.012	2.078	2.092
Pd_2-C_2	1.997	2.060	2.048
Pd_1-C_3	2.006	2.032	2.031
Pd_2-C_4		2.032	2.031
C_1-O_1	1.158	1.158	1.151
C_2-O_2	1.166	1.158	1.166
C_3-O_3	1.145	1.137	1.138
C_4-O_4		1.137	1.138
Pd_1-Cl_1	2.429	2.368	2.371
Pd_1-Cl_3			
Pd_2-Cl_2	2.379		2.371
Pd_2-Cl_4	2.382	2.368	
	Bond Angles		
$Pd_1-C_1-O_1$	132.4	140.9	138.3
$Pd_1-C_{2-}-O_2$	130.3	134.6	137.2
$Pd_1-C_3-O_3$	171.2	173.0	174.1
$Pd_2-C_1-O_1$	144.3	134.6	138.3
$Pd_2-C_2-O_2$	144.6	140.9	137.2
$Pd_2-C_4-O_4$		173.0	174.1
$C_1-Pd_1-C_2$	88.8	93.2	94.1
$C_1-Pd_2-C_2$	95.7	93.2	94.1
$C_3-Pd_1-C_2$	95.0	93.0	93.5
$C_2-Pd_2-C_4$		93.0	93.5
$Cl_1-Pd_1-C_3$	86.7	86.2	84.9
$Cl_3-Pd_1-C_2$			
$Cl_2-Pd_2-C_1$	85.8	-	87.4
$Cl_2-Pd_2-C_4$			84.9
$Cl_4-Pd_2-C_4$		86.2	
$Cl_1-Pd_1-C_1$	89.7	87.8	87.4
$Cl_4-Pd_2-C_2$	85.5	87.8	
$Cl_1-Pd_1-Cl_3$			
$Cl_2-Pd_2-Cl_4$	93.0		

Table 4. Wiberg Bond Indices Calculated at the DFT/B3LYP Level

bond	**2′**	**5′**	**7a**	**7b**
Pd_1-Pd_2	0.153	0.127	0.118	0.118
Pd_1-C_1	0.522	0.380	0.444	0.410
Pd_1-C_2	0.522	0.444	0.444	0.481
Pd_2-C_1	0.522	0.515	0.444	0.410
Pd_2-C_2	0.522	0.537	0.447	0.481
Pd_1-C_3		0.499	0.452	0.459
Pd_2-C_4			0.452	0.459
C_1-O_1	2.030	2.105	2.115	2.176
C_2-O_2	2.030	2.039	2.115	2.055
C_3-O_3		2.195	2.270	2.267
C_4-O_4			2.270	2.267
Pd_1-Cl_1	0.302	0.282	0.347	0.343
Pd_1-Cl_4	0.302			
Pd_2-Cl_2	0.302	0.365		0.343
Pd_2-Cl_3	0.302	0.368	0.347	

Wiberg Indices Analysis. We report in Table 4 the Wiberg bond indices for each complex. In all cases, the Wiberg bond index of the Pd−Pd hypothetical direct bond is very small. Although the Pd−Pd distances compare well with that observed in the Pd bulk (2.75 Å), this indicates there is practically no Pd−Pd direct bond. This result is consistent with the detailed multireferential study discussed above. On the other side, the bond index between the palladium atoms and the C_1 and C_2 carbon atoms of the

Table 5. NBO Charge Distributions in Pd(I) Complexes Calculated at the DFT/B3LYP Level

	2′	5′	7a	7b
Pd_1	+0.429	+0.328	+0.377	+0.382
Pd_2	+0.429	+0.469	+0.377	+0.382
Cl_1	−0.684	−0.639	−0.524	−0.524
Cl_2	−0.684	−0.576		−0.524
Cl_3	−0.684	−0.574		
Cl_4	−0.684		−0.524	
C_1	+0.420	+0.418	+0.402	+0.424
C_2	+0.420	+0.398	+0.402	+0.368
O_1	−0.480	−0.427	−0.411	−0.371
O_2	−0.480	−0.471	−0.411	−0.449
C_3		+0.543	+0.570	+0.570
C_4			+0.570	+0.570
O_3		−0.469	−0.414	−0.415
O_4			−0.414	−0.415
$q(C_1O_1)$	−0.060	−0.009	−0.009	+0.053
$q(C_2O_2)$	−0.060	−0.073	−0.009	−0.081
$q(C_3O_3)$		+0.074	+0.156	+0.155
$q(C_4O_4)$			+0.156	+0.155

Table 6. Natural Orbital Occupancies of CO π^* Orbitals

	2′	5′	7a	7b
C_1O_1	0.528	0.520	0.470	0.406
C_2O_2	0.528	0.452	0.470	0.534
C_3O_3		0.172	0.137	0.135
C_4O_4			0.137	0.135

bridging COs are significant (0.5); this confirms the CASSCF-DDCI+PT2 result showing that the Pd−Pd interaction in **2′** arises via the bridging carbonyls. It is interesting to note that the Wiberg index related to the Pd−C bonds is nearly independent of the position (bridging or terminal) of the carbonyl groups.

Charges Densities: σ Donation and π Back-Donation. To have a better understanding of the nature of the Pd−CO bonds in each complex, we have more precisely studied the electron densities on the carbonyl groups. Indeed, their relative positions (bridging or terminal) significantly change their local properties, e.g., their vibrational stretching wavenumbers.

The NBO charges are given in Table 5. The positive charge of the Pd atoms varies from 0.33 to 0.47, depending on the electronic environment of each palladium. Globally, the charge is larger when Pd is bound to two chlorines than to one chlorine (larger Pd−Cl polarization). Palladium charges in both cis and trans disubstituted complexes are very similar.

The most interesting fact concerns the charges localized on the carbonyls. The total charge of the bridging COs is slightly negative (the global electronic transfer is always directed from the palladium to the carbonyls) except for C_1O_1 in the cis compound (**7b**). For the terminal carbonyls, the charge transfer is very different, the total charge of CO being always positive.

Looking at the distribution of electron density between the carbon and the oxygen atoms inside CO, it appears that a large polarization occurs. Thus, the charge-transfer process is more complex, because such polarization comes from the fact that part of the electrons go from Pd to CO molecular orbitals mostly localized on O (back-donation) while another part go from CO molecular orbitals mostly localized on C to Pd (donation). To quantify the back-donation process, we give in Table 6 the computed electron populations of the CO π^* orbitals for each complex. Clearly, the process is much more important in bridging COs than in terminal COs (factor 2). We can then expect that the CO bond strength will be decreasing in the bridging CO, whereas it will be unchanged or slightly increasing in the terminal CO. This is well-correlated with the respective Wiberg indices and CO bond lengths of bridging and terminal carbonyls.

Carbonyl Vibrational Analysis. Theoretical calculations within the harmonic approximation as well as experimental data concerning the wavenumbers and the corresponding intensities of the CO stretching modes are given in Table 7 for complexes **2′** and **5′**. Theoretical results concerning the two substituted **7a** and **7b** species are given in Table 8.

Experimental values of the wavenumbers for bridging carbonyls in **2′** and **5′** are reduced by about 200 cm^{-1} compared to the gas-phase value (2143 cm^{-1}), reflecting a significant π^* back-donation from the palladiums to the bridging carbonyls. B3LYP-calculated values are larger than the experimental ones by nearly 50 cm^{-1} in **2′** and 80 cm^{-1} in **5′**. We could expect that a shift of 65 cm^{-1} from theoretical to experimental values is mainly due to the choice of the DFT approach, which generally overestimates the vibrational energies. One should note that almost the same overestimation is observed for the vibration of free CO, for which the DFT/B3LYP calculated wavenumber is equal to 2207 cm^{-1}, whereas the experimental value is 2143 cm^{-1}. Despite this constant discrepancy, the difference between the symmetric and antisymmetric wavenumbers is in perfect agreement with experimental data. Concerning the terminal carbonyl in **5′**, the higher value of the stretching wavenumber compared to that of the bridging COs reflects a weaker π^* back-donation (see Table 6). The calculated value compares well with the experimental data, taking into account the overestimation due to the DFT approach. The analysis of the various intensities attributed to each vibrational transition in **2′** and **5′** is strongly correlated to the spatial symmetry of each compound as well as to their permanent dipole moment. In compound **2′**, the

Table 7. Theoretical and Experimental Stretching Wavenumbers ν (cm^{-1}) and Relative Intensities (km mol^{-1}) of the Bridging and Terminal CO Vibrations for 2′ and 5′[a]

		2′			5′		
		DFT/B3LYP	expt solid 2	expt. liquid	DFT/B3LYP	expt. solid **5**	expt. liquid
bridging CO	asym	1956 (783)	1903 (s)	1906 (s)	1[b] 1980 (636)	1903 (s)	1907 (s)
	sym	2012 (89)	1964 (w)	1968 (w)	2[b] 2049 (265)	1964 (w)	1968 (w)
	$\Delta\nu_{sa}$	56	61	62	69	60	61
terminal CO					2157 (599)	2114 (vs)	2132 (s)

[a] Relative intensities are given in parentheses. [b] Normal coordinates are localized on C_1O_1 and C_2O_2, respectively.

Table 8. DFT/B3LYP-calculated Stretching Wave Numbers ν (cm^{-1}) and Relative Intensities (km mol^{-1}) of the Bridging and Terminal CO Vibrations for **7a** and **7b**[a]

	7a	**7b**
	Bridging CO	
	asym 2015 (819)	1[b] 1986 (621)
	sym 2060 (55)	2[b] 2087 (258)
$\Delta\nu_{sa}$	45	101
	Terminal CO	
	asym 2213 (815)	asym 2210 (502)
	sym 2219 (18)	sym 2217 (330)
$\Delta\nu_{sa}$	6	7

[a] Relative intensities are given in parentheses. [b] Normal coordinates are localized on C_1O_1 and C_2O_2, respectively.

Table 9. Dipole Moments (D)[a] Calculated at the DFT/B3LYP Level

	2′	**5′**	**7a**	**7b**
μ_X	0.0	−5.27	0.0	0.0
μ_Y	0.0	3.32	0.0	6.29
μ_Z	2.41	1.40	−0.10	0.42
$\lvert\mu\rvert$	2.41	6.38	0.10	6.31

[a] Cartesian axes are defined in Figure 1; *x* along Pd_1-Pd_2 and *y* along C_1-C_2.

symmetry group is C_{2v} and both vibrations can be labeled as symmetric and antisymmetric normal modes delocalized on each CO. A priori, both transitions are allowed, and thus no selection rules can be applied in this case. Nevertheless, we can see from Table 7 that the antisymmetric mode is much more active than the symmetric mode. In fact, both vibrations are nearly perpendicular to the permanent dipole moment, which is along the *z* axis (the angle between the CO directions is 137°). We can thus conclude that the change in the dipole moment (which is directly correlated to the intensity) is much smaller for the symmetric mode than for the antisymmetric mode. In compound **5′**, the symmetry group is C_1 and no more spatial symmetry exists. In that case, the normal modes of the bridging carbonyls are nearly localized on each CO. The corresponding transitions are allowed, each of the modes nearly lying in the *xy* plane (the angle between the bridging COs directions being 142°) as well as the principal components of the dipole moment (Table 9). Theoretical results are in agreement with the qualitative experimental intensities.

In the trans **7a** and cis **7b** complexes, vibrational wavenumbers of the bridging carbonyls show that the π^* back-donation is significant and of the same order as in complexes **2′** and **5′**. In the trans geometry (C_2 symmetry), we have one symmetric and one antisymmetric normal mode. Both vibrational transitions are allowed. However, the CO directions are nearly perpendicular to the C_2 (*z*) axis (the angle between the two CO directions is equal to 149°). Hence, the symmetric vibration has a very small effect on the permanent dipole moment, which lies along the C_2 axis with a very low magnitude. Its intensity is 15 times smaller than that of the antisymmetric mode. The cis complex is of C_s symmetry (*yz* plane); both bridging CO vibrations are decoupled and are symmetric modes. For each vibration, the π^* back-donations are quite different, leading to a wavenumber gap of 101 cm^{-1}, which reflects the different surroundings of each carbonyl. Both infrared transitions are allowed, and their intensities are on the same order of magnitude (factor 2), because the vibrational mode lies almost along the *x* axis, as does the permanent dipole moment (see Table 9). The terminal carbonyls in both systems belong to different irreducible representations of the symmetry group; in the trans complex, symmetric (A) and antisymmetric (B) normal modes lead to vibrational wavenumbers almost unchanged with respect to the free CO. They correspond to a very small π^* back-donation (see Table 6), three times smaller than in the bridging CO case. Furthermore, both vibrations are quasidegenerate (6 cm^{-1}) because both carbonyls are well-separated. The same remarks hold for the symmetric (A′) and antisymmetric (A″) normal modes of the cis complex, in which the π^* back-donation is on the same order of magnitude and the two terminal COs have no direct interaction. On the contrary, the behavior of the intensities of the IR transitions in both systems is quite different. In **7a** (trans), the symmetric mode transition is nearly forbidden because of a very small permanent dipole moment located along the *z* axis, whereas the vibration arises close to the *xy* plane (the angle between CO axes being 157°). In the case of **7b**, both vibrations and dipole moment are in the same plane (*xy*), so IR intensities are on the same order of magnitude (less than a factor of two).

Table 10. Comparison of the r_{CO} Bond Lengths and ν_{CO} Wavenumbers in the Pd(I) Complexes with Those of Free CO Calculated at the DFT/B3LYP Level

	2′	**5′**	**7a**	**7b**
		Δr_{CO} (Å)		
C_1O_1	+0.026	+0.017	+0.017	+0.010
C_2O_2	+0.026	+0.025	+0.017	+0.025
C_3O_3		+0.004	−0.004	−0.003
C_4O_4			−0.004	−0.003
		$\Delta\nu_{CO}$ (cm^{-1})		
C_1O_1	−251 (−267)[a]	−227 (−267)	−192	−221
C_2O_2	−195 (−202)	−158 (−206)	−147	−120
C_3O_3		−50 (−55)	+6	+3
C_4O_4			+12	+10

[a] Values in parentheses are from experimental spectra (this work).

4. Conclusion

The dianionic dipalladium(I) complex $[Pd_2(\mu\text{-}CO)_2Cl_4]^{2-}$ reacts readily with methoxy- or acetato compounds or with carbon monoxide, and the substitution process affects one or two of the chloro ligands so that the $Pd_2(\mu\text{-}CO)_2$ core is maintained. Calculations have been carried out to understand the nature of the bond between the two d^9 palladium atoms and the reasons for the high bridging or terminal carbonyl IR wave numbers. The question of the magnetism of the Pd (d^9) atom has also been addressed. CASSCF and (CAS + DDCI) calculations have been performed in order to take into account the charge fluctuation between the d_{xy} orbitals bearing two electrons. It has been shown that the pairing of these two electrons is due to the delocalization along the CO bridging ligands. More precisely, the corresponding occupied MO is antibonding between the two d_{xy} orbitals of the Pd atoms and bonding within the π^* MO of the CO groups. It follows that the correlated wave function has an important weight on a single determinant and that the DFT

approach can reasonably be used to perform a vibrational analysis of the CO ligands stretching modes. Table 10 clearly shows the strong correlation existing between variations of CO bond lengths and CO stretching wavenumbers in the Pd(I) complexes. Furthermore, the spatial symmetry of each of the compounds allowed us to make a simple explanation about the intensities of the various vibrational bands.

Acknowledgment. S.B. thanks Rhône-Poulenc for financial support during her Ph.D. thesis. We also acknowledge Prof. Pablo Espinet (Universidad de Valladolid, Spain) for helpful discussions.

IC050910N